CHEM**CAT**CHEM
Concepts

VIP *Very Important Paper*

Single-Particle Studies to Advance the Characterization of Heterogeneous Biocatalysts

Ana I. Benítez-Mateos,[a] Bernd Nidetzky,[b, c] Juan M. Bolivar,[b] and Fernando López-Gallego*[a, d]

Immobilized enzymes have been widely exploited because they work as heterogeneous biocatalysts, allowing their recovery and reutilization and easing the downstream processing once the chemical reactions are completed. Unfortunately, we suffer a lack of analytical methods to characterize those heterogeneous biocatalysts at microscopic and molecular levels with spatio-temporal resolution, which limits their design and optimization. Single-particle studies are vital to optimize the performance of immobilized enzymes in micro/nanoscopic environments. In this Concept article, we review different analytical techniques that address single-particle studies to image the spatial distribution of the enzymes across the solid surfaces, the sub-particle substrate diffusion, the structural integrity and mobility of the immobilized enzymes inside the solid particles, and the pH and O_2 internal gradients. From our view, such sub-particle information elicited from single-particle analysis is paramount for the design and fabrication of optimal heterogeneous biocatalyst.

1. Introduction

Organic chemists and chemical industries are lastly embracing biocatalysis as a key enabling technology to access more complex synthetic schemes in a more sustainable manner.[1, 2] However, the use of enzymes as isolated soluble catalysts suffers the limitations of the homogeneous catalysis where product purification is arduous and the catalysts are hardly reused.[3] Furthermore, the enzymes have been majorly evolved to work under mild conditions (room temperature, neutral pH, atmospheric pressure) within the crowded environment of the cell milieu, thus their stability becomes an issue when the chemical process demands harsh and diluted reaction conditions.[4] Enzyme immobilization is an old solution for both the solubility and the stability of the enzyme. Paraphrasing DiCosimo et al.,[3] the immobilized enzymes are essentially a specialized form of heterogeneous catalysts -heterogeneous biocatalysts- that can be recovered and reused, often retain activity for long periods and are amenable to a wide variety of reactor designs, including flow-reactor for continuous processes. Nevertheless, the immobilization of enzymes on solid materials poses some limitations such as mass transfer issues, internal gradients (pH, temperature, substrates, etc.) and negative effects that the immobilization itself causes on the enzyme properties.[3, 5]

To overcome those drawbacks, advanced analytical tools should support the better comprehension of the effects caused by the immobilization on the enzyme performance. In this context, like in heterogeneous catalysis,[9–11] spatio-temporal characterization of heterogeneous biocatalysts contributes to their optimization. Hence, understanding how enzymes work inside a solid particle makes the fabrication of heterogeneous biocatalysts more rational. Unfortunately, enzyme immobilization is a still trial-and-error approach where characterization studies are still based on observable parameters at macroscopic level.[5, 12] These averaged measurements are collected from information gathered at the liquid bulk solution without considering the spatial heterogeneity of the sample. Thus, these macroscopic studies hardly reveal the spatio-temporal performance and the intraparticle environments of the heterogeneous biocatalysts. Like inside the living cells, the enzymatic systems supported on porous materials are dynamics, therefore analytical studies with spatio-temporal resolution can provide essential information about the properties of the heterogeneous biocatalysts at single-particle level. These techniques can reveal the structural rearrangements undergone by the immobilized enzymes with spatio-temporal resolution, the 3D-organization of cell-free biological systems, the mass transport fluctuations of the reactants and the reaction kinetics inside the microstructure of the porous materials under operando conditions (Figure 1).

As in heterogeneous chemical catalysis,[13] single-particle studies reveal how the spatial heterogeneity of the solid

[a] A. I. Benítez-Mateos, Dr. F. López-Gallego
Heterogeneous Biocatalysis Group
CIC BiomaGUNE
Paseo Miramon 182, San Sebastian-Donostia, 20014 (Spain)
E-mail: flopez.ikerbaske@cicbiomagune.es

[b] Prof. B. Nidetzky, Dr. J. M. Bolivar
Institute of Biotechnology and Biochemical Engineering
Graz University of Technology
NAWI Graz, Petersgasse 12, 8010 Graz (Austria)

[c] Prof. B. Nidetzky
Austrian Centre of Industrial Biotechnology
Petersgasse 14, 8010 Graz (Austria)

[d] Dr. F. López-Gallego
IKERBASQUE, Basque Foundation for Science
Bilbao (Spain)

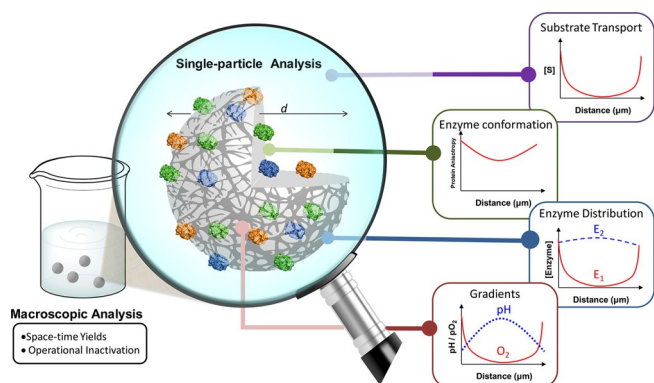The ORCID identification number(s) for the author(s) of this article can be found under https://doi.org/10.1002/cctc.201701590.

Figure 1. Schematic representation of the information provided by single-particle analysis of heterogeneous biocatalysts. Conformation and localization of enzymes, substrates and products mass transport and pH and O₂ gradients can be determined within the solid particles with spatial and temporal resolutions.

materials (material defects,[14] size dispersion,[15] functional patterning,[16] etc.) influence the final properties of the immobilized enzymes. Therefore, insights in protein conformation, mass transfer effects and enzyme kinetics at the micro/nano-scale within a single-particle contribute to understand the observable productivity and stability of the heterogeneous biocatalysts determined by macroscopic analysis (Figure 1).[17,18] In the last two decades, single-molecule[19] and single-cell[20] studies have paved the way to better understand the dynamics of biological processes and aided synthetic biology to succeed in different biotechnological applications. These studies have not only released fundamental biological and biochemical knowledge but also provided analytical tools that shine light on protein localization, protein conformations and metabolite transport within the cellular microenvironment. These studies show the immense technical possibilities existing for microscopic characterization of porous particles, which are by far simpler and better controllable than living cells. Although the intraparticle characterization of heterogeneous biocatalysts has received much less attention, single-particle studies are gaining popularity between the biocatalysis community to characterize the internal properties of ready-to-use heterogeneous biocatalysts just before their operational evaluation.[17] Particularly, these studies are rather important in flow-biocatalysis; a topic that is intensively investigated nowadays.[20] Unfortunately, methods to imaging the performance of the immobilized enzymes in flow-reactors[21] (monoliths, microfluidic channels, packed-beds) are scarce, since looking inside the reactors while they are operating is rather more challenging than studying the isolated particles under the microscope.

In this Concept article, we outline some of the most relevant advances for the characterization of heterogeneous biocatalysts at single-particle level. We will review different analytical techniques that elicit the spatial organization, the kinetics and the stability of immobilized enzymes within solid particles, as well the mass transport of reagents and the pH and oxygen gradients inside the porous microstructure during the bioprocesses. This revision ultimately aims to stress the importance

of single-particle analysis as driving force to optimize enzyme immobilization proceedings. From our view, the information elicited from the interior of the particles is paramount for the design and fabrication of optimal heterogeneous biocatalysts.

2. Single-Particle Spatial Distribution of Immobilized Enzymes Across Solid Carriers

The three-dimensional distribution of immobilized enzymes on solid carriers plays a critical role in the study of the biocatalyst activity and its reaction kinetics (Figure 1). However, the enzymes have been traditionally assumed to be homogeneously distributed across the surface of solid carriers. In fact, most of immobilization procedures lack the control of both the orientation and the spatial distribution of the enzymes, resulting in the misinterpreting effects underlying the conventional characterization of heterogeneous biocatalysts. In this context, the preparation of immobilized enzymes demands new methodologies to elicit the spatial organization of enzymes across the microstructure of the solid carriers.[20,23] Over the past few decades, atomic force microscopy (AFM),[24,25] low-temperature field-emission scanning electron microscopy (Cryo-FESEM),[26] spherical aberration (Cs)-corrected STEM,[27] infrared and fluorescence spectroscopy among others, have emerged for inquiring into the spatial distribution of immobilized proteins across the solid surfaces. Micro-Infrared and micro-RAMAN spectroscopies image the spatial distribution of label-free enzymes across solid carriers (particles 20–200 μm), unveiling microscopic information of ready-to-use heterogeneous biocatalysts.[28,29] However, fluorescence studies using confocal laser scanning microscopy (CLSM) are most widely preferred, owing to its high resolution and versatility.[30,31] In this field, many techniques are available to study the distribution of fluorophore-labeled proteins, from a single molecule to a multi-enzymatic system.

All proteins, and consequently all enzymes, show intrinsic fluorescence in the UV region of the spectrum, owing to the presence of three fluorescent amino acids (tyrosine, tryptophan and phenylalanine) in their primary sequence.[32] This strategy is mainly exploited to study protein conformational changes of the both soluble and immobilized enzymes.[33] Mapping the proteins by recording their intrinsic fluorescence would be ideal because this technique would be universal and not require any labeling, however, as far as we know, none example has been reported yet.

The main strategy to analyze the spatial distribution of enzymes across solid surfaces is based on fluorophore-labeled proteins. The fluorophores can be either genetically encoded (e.g. fluorescent proteins)[34] or organic labels (e.g. fluoresceine).[35] Bolivar et al. exploited fluorescent proteins to modulate the protein distribution across porous agarose beads (50–150 μm).[36] This work demonstrates that the immobilization rate controls the protein distribution, observing uniform and not uniform protein distributions when the immobilization was slow and rapid, respectively. The immobilization rate can be easily modulated by controlling the immobilization chemistry (nature and density of the reactive groups) and the

immobilization conditions (presence of competitors, pH, temperature). On the other hand, the single-particle studies of green fluorescent protein tagged with a lectin domain allowed monitoring the spatial distribution of the immobilized proteins over the time.[37] This study revealed that protein is primarily immobilized on the outer surface of porous agarose beads, but then gradually colonizes the whole microstructure of the agarose particle (50–150 μm) along 30 minutes. These results evidence that the interactions between the agarose surface and the lectin domain are dynamic and suggest an intraparticle association/dissociation equilibrium between the lectin and the sugars forming the agarose fibers. Such equilibrium seems to enable the reorganization of the spatial distribution inside the particles upon the immobilization.

However, when using non fluorescent proteins, chemical labeling with chemical fluorophores is an excellent solution to study the spatial distribution of immobilized enzymes.[38] The chemical labeling of several enzymes with different fluorophores have been successfully exploited to determine the spatial organization of multi-enzyme systems immobilized on solid carriers with different architectures.[39–41] The understanding of the spatial organization of multi-enzyme systems immobilized on solid carriers is required to optimize the multi-functional heterogeneous biocatalysts in order to perform cascade reactions more efficiently. Rocha-Martín et al.[40] tuned the sub-particle spatial distribution of two alcohol dehydrogenases by modulating their immobilization rates according to a previous work[36] (Figure 2).

As result, they observed that uniform co-localization of two enzymes enhances the in situ NADH recycling efficiency during the operation of a bio-redox cascade. The sub-micrometric proximity of the two dehydrogenases presumably exerts some cooperation effects that explain the low apparent K_M values towards NADH, even lower than the ones presented by the soluble system, pointing out a concentration effect in the NADH pool within the porous surface.[40] These results reveal the high relevance of single-particle analysis of protein distribution on the performance of heterogeneous biocatalysts. Therefore, the control of enzyme spatial organization is clue for improving the biotechnological processes catalyzed by heterogeneous systems.

3. Single-Particle Reaction Kinetics of Immobilized Enzymes

Monitoring and imaging the enzyme activity during the operational process (in operando studies) at the nano/microscale can directly provide information that would be inaccessible otherwise. In a recent paper, Harada et al. exploited high-speed atomic force microscopy to measure in operando the conformational changes of the cellobiose dehydrogenase immobilized on flat gold surfaces functionalized with heme groups.[42] This work sheds light on the mechanism of this multi-domain protein at nanometric scale. The highly specialized infrastructure required for these studies makes that spatial resolution studies monitoring the catalytic activity of the immobilized enzymes are dominated by fluorescence
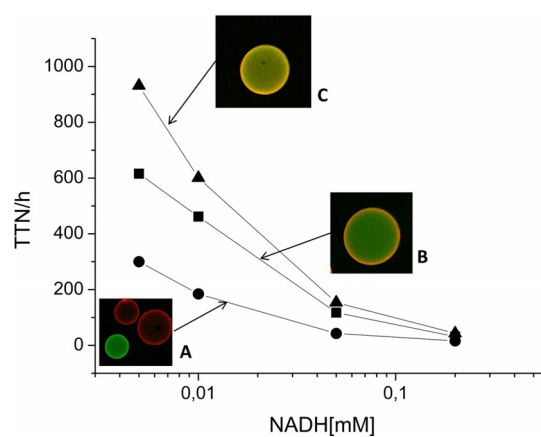

Figure 2. Effect of enzyme distribution inside agarose particles (50–150 μm) on the cofactor-recycling frequency. Alcohol dehydrogenase (Tt27-ADH2) and Glutamate dehydrogenase (Tt27-GDH) labeled with fluorescamine (green) and rhodamine B (red) respectively, performed a bio-redox cascade. The main dehydrogenase Tt27-ADH2 catalyzed the asymmetric bio-reduction of 2,2,2-trifluoro-acetophenone into (S)-a-(trifluoromethyl) benzyl alcohol with NADH consumption. Orthogonally, NADH-recycling reaction was performed by Tt27-GDH by using ʟ-glutamate as sacrificing substrate. A) The two enzymes were separately immobilized on different agarose-Ni^{2+}/Glioxil particles (AG-Ni^{2+}/G):Tt27-GDH was immobilized in one batch by using IMAC chemistry, whereas Tt27-ADH2 was immobilized in a different batch by using glyoxyl chemistry. The two batches were mixed to perform the reaction (circles). B) The two labeled enzymes were sequentially co-immobilized onto the same AG-Ni^{2+}/G particle through different bonding chemistries: Tt27-GDH presented a not uniform distribution while Tt27-ADH2 showed a uniform one (squares). C) The two enzymes were homogeneously co-immobilized onto the same AG-Ni2+/G particle (triangles). In this case,Tt27-GDH was first immobilized in the presence of 0.2 ᴍ imidazole, which hindered the immobilization and enabled a more homogeneous distribution of the enzyme. Second, Tt27-ADH2 was sequentially immobilized through aldehyde chemistry. Reproduced from [40] with permission of Wiley.

spectroscopy; a worldwide and highly accessible technique. In the last decades, many advances[43–48] in development of fluorescence-based reporter systems have boosted the spatio-temporal resolution and sensitivity of analytical methods to study a broad range of dynamic processes during the catalytic reactions. In this context, many fluorogenic substrates are commercially available as useful reporter systems.[48] These fluorogenic substrates can be enzymatically transformed into fluorescent products that can be read out to assess the system kinetics (Figure 3).[45,49–53] Particularly, CLSM is a very powerful technique for enzymology when enzymes are immobilized and allows recording the local production of products.[54]

One of the first studies to evaluate the kinetics of immobilized enzymes using fluorogenic substrates was the real time DNA sequencing.[55] The well-known real-time DNA sequencing was performed using a DNA polymerase immobilized on a zero-mode waveguide (ZMW) pore (100 nm) of a glass surface and fluorescently labeled nucleotides. The growth of the DNA chain was monitored by fluorescent bursts after incorporation of the fluorescent nucleotides. More recently, Velonia et al. demonstrated that single-particle enzyme kinetics can be monitored at real-time using CLSM as well. They used a industrially relevant enzyme (lipase from *Candida antarctica B; CALB*)[56] immobilized on a glass surface derivatized with
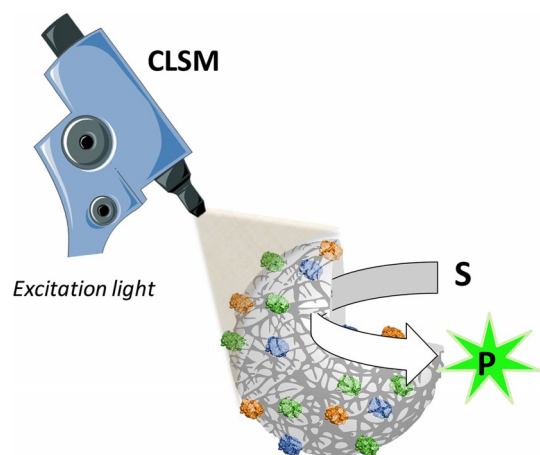
Figure 3. Schematic representation of single-particle measurements of enzyme reaction kinetics monitored by CLSM and using fluorogenic substrates.

Figure 4. On line monitoring of single-particle kinetics by fluorogenic substrates. (A-C) Confocal microscopy images of the co-immobilized HRP (labeled with rhodamine B, red) and GOx (labeled with FITC, green) in nanocrystal complexes. A) GOx was firstly immobilized by precipitation with metal complexes. Then, HRP was absorbed to the precipitate surrounding the nanocrystal complex. B) HRP was precipitated and GOx was superficially absorbed to the nanocrystal complex. C) Both enzymes were precipitated with metals obtaining a random distribution. D) The cascade reaction catalyzed by GOx and HRP using fluorogenic substrates. E) Confocal images showing the transport of a fluorescent glucose analogue (6-NBDG) from outside to inside in the biocatalytic system GOx@HRP. F) Confocal images showing the transport of resorufin from inside to outside of GOx@HRP. Adapted from [41] with permission of Royal Society of Chemistry.

hydrophobic groups. A fluorogenic substrate was hydrolyzed by the immobilized CALB yielding a fluorescent product. These studies revealed that the enzymes absorbed on a hydrophobic surface presented a kinetic variability attributed to the existence of different active enzyme conformations across the solid surface as result of the random immobilization mechanism. This sort of studies may provide spatial resolution to the kinetic behavior of the immobilized enzymes by imaging those locations where enzyme performance is altered.

Fluorogenic substrate-based strategies have served as a springboard to investigate more complex biological systems where multi-enzyme cascades are involved. Many factors as enzymatic cooperation, reactants transport, spatial distribution, etc., must be considered when studying multi-enzyme systems due to their intrinsic molecular complexity. The reaction kinetics of the immobilized multi-enzyme system formed by glucose oxidase (GOX) and horseradish peroxidase (HRP) are the most studied at single-particle level by far.[41,45,57–59] These two enzymes have been co-immobilized on a large variety of surfaces through a diversity of immobilization chemistries. Normally, a fluorogenic substrate (i.e Amplex red) is oxidized by HRP yielding a fluorescent product (i.e Resorufin) only in presence of the hydrogen peroxide that is in situ produced as by-product from the oxidation of glucose catalyzed by GOX. Li et al. co-immobilized these two enzymes on copper-phosphate particles (10 μm) with different spatial distributions.[41] The cascade worked more efficiently when the HRP was spatially confined inside the particles and the GOX was attached to the outer surface (Figure 4 A–C). A similar enzyme cascade was co-immobilized on porous polymer monoliths by a photopatterning method, demonstrating again the importance of the spatial organization of the enzymes for continuous operation under flow conditions.[21]

By using two fluorogenic substrates, they observed that the fluorogenic glucose is firstly concentrated and oxidized in the outer surface where the GOX is located, while the fluorescent resoruf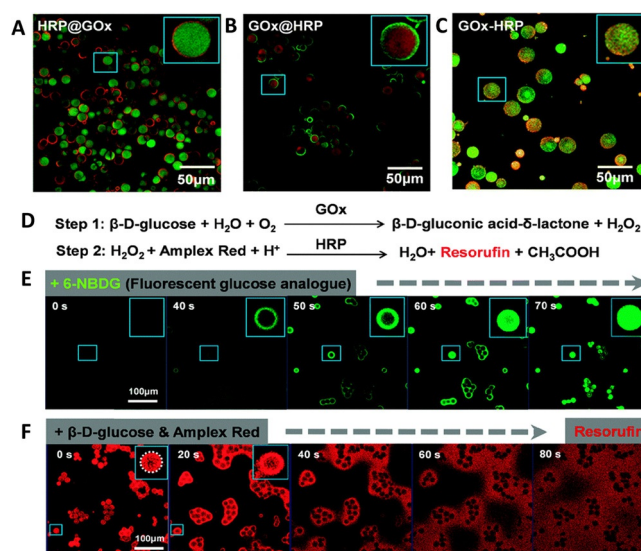in initially appears inside the particles where HRP was located and then gradually diffused out to the bulk (Figure 4 D–F).

In a more sophisticated architecture, several enzymes are compartmentalized into different polymersomes (100–300 nm) as sub-compartments within larger particles (60 μm) or oil-water droplets (80–1000 μm).[57,60] This approach was applied for different multi-enzyme systems that catalyze sequential cascade reactions whose final product is fluorescent. The single-particle studies elicited the spatial distribution of the multi-enzyme system by imaging, after 3D computational reconstruction, the fluorescence spots where the final product is primarily accumulated before diffusing across the microstructure of the larger particle (Figure 5). Those spots correspond to the polymersomes where the enzyme that catalyzes the last reaction of the sequential cascade is sub-compartmentalized.[57,60] The accumulation of the fluorescence into the polymersome is explained by the electrostatic entrapment of the product that prevents its rapid diffusion to other compartments within the micrometric polymersome and to the reaction bulk. Additionally, the accumulation of the final product in the compartments where the last enzyme is located also demonstrates an external transport of the substrate and inter-compartment diffusion of the intermediates. These single-particle studies point out that the ordered transport of the substrates is the consequence of the spatial distribution of the multi-enzyme system co-immobilized on the solid materials.
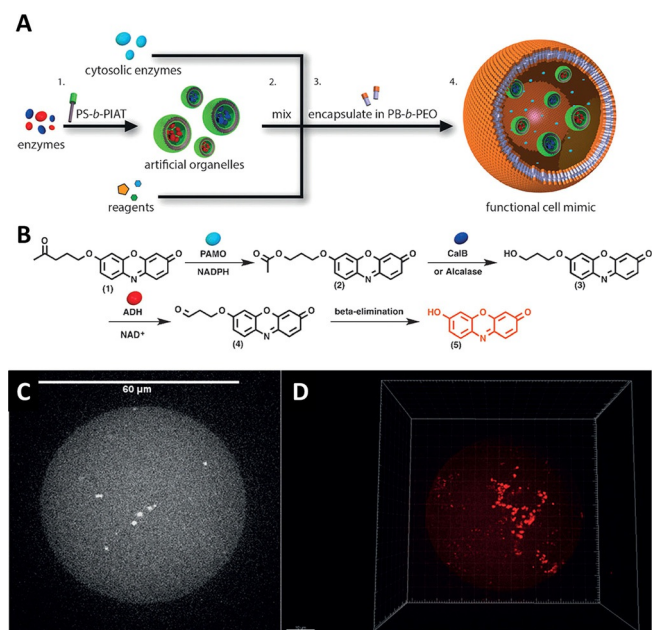
Figure 5. Single-particle studies of an encapsulated multi-enzymatic cascade by fluorescence microscopy. A) Initially the different enzymes were encapsulated in polystyrene-b-poly(3-(isocyano-alanyl-amino-ethyl)-thiophene) (PS-b-PIAT) polymersomes 1); Then, the organelles-like polymersomes (100–300 nm) were mixed with other cytosolic enzymes and reagents 2); followed by their encapsulation in polybutadiene-b-poly(ethylene oxide) (PB-b-PEO) vesicles 3); to finally create a functional cell mimic (60 μm) containing the immobilized multi-enzymatic cascade. B) Multi-enzymatic reaction cascade inside organelles-like nanoreactors. Profluorescent substrate (1) is catalyzed by phenylacetone monooxygenase (PAMO) with one unit of NADPH being consumed, to yield ester (2), which is subsequently hydrolyzed by the enzyme lipase B from *Candida antarctica (CalB)* or the enzyme alcalase to provide a primary alcohol (3). Alcohol dehydrogenase (ADH) oxidizes the alcohol, by using the cofactor NAD+, to give aldehyde (4) which then undergoes spontaneous beta-elimination to be converted into resorufin (5) as the final fluorescent product. C) Enhanced spinning disk confocal fluorescence imaging at single particle level of a cell mimic after production of resorufin. The fluorescent product is easily observable like spots in the compartmentalized organelles. D) The 3D representation of the polymersome where the organelles producing resorufin are highlighted. Adapted from [60] with permission of Royal Society of Chemistry.

Cofactor-dependent enzymes (e.g. NADH-dependent reductases and oxidases, FAD-dependent oxygenases) catalyze many interesting reactions in industrial biocatalysis.[58–60] Many of these cofactors present auto-fluorescence that can be monitored during the enzymatic activity. Unlike the soluble enzymes where single-enzyme dynamics in presence of cofactors have been reported more extensively,[61] monitoring the cofactor utilization by immobilized enzymes with spatial resolution is underexploited. FAD is an excellent cofactor for these studies because the cofactor-enzyme electron transfer causes fluorescence fluctuations that can be attributed to different cofactor conformations and states. Nevertheless mapping of those fluctuations remains unknown.[65] These single-molecule studies have served to advance in the understanding of the kinetics of cofactor-dependent enzymes observed in bulk studies.[65,66] In addition, the effect of the reaction conditions and mass transport restrictions on the enzyme activity can be studied with

spatial resolution by mapping the cofactor utilization within the solid phase.[67–69] In this regard, nicotinamide cofactors whose fluorescence intensity is higher for the reduced form (NAD(P)H) than for the oxidized one (NAD(P)+) have been very useful to evaluate the activity of different immobilized alcohol dehydrogenases (ADH) under different operational conditions. Using soluble NAD+, O'Brien[70] et al. created artificially local pH gradients with microelectrodes and monitored the local activity of an immobilized alcohol dehydrogenase. Imaging the cofactor fluorescence, the authors demonstrated that only those enzymes surrounded by alkaline pH environment were able to efficiently reduce NAD+ to NADH using ethanol as substrate. This effect was observed with enzymes immobilized on both glass surfaces and porous beads.

On the other hand, cofactor and enzymes can be co-immobilized to fabricate self-sufficient heterogeneous biocatalysts that do not require exogenous supply of cofactor. Even though the concept of self-sufficient heterogeneous biocatalyst has been exploited for a dozen of cascade reactions,[40,71–74] the cofactor utilization inside the solid particles has been rarely studied. Velasco-Lozano et al.[69] have mapped the cofactor utilization within porous agarose particles that co-immobilize the main enzyme (alcohol dehydrogenase), the cofactor recycling enzyme (formate dehydrogenase) and the cofactor (NAD+). In operando studies by means of fluorescence microscopy demonstrate that the co-factor is catalytically available for the co-immobilized enzymes and in situ recycled inside the porous surface without diffusing out to the reaction bulk (Figure 6).

Finally, single-particle fluorescence studies have also provided valuable information about the kinetics of cell-free protein synthesis (CFPS) systems; a highly complex biological machinery. In these systems, both transcriptional and translational machineries have been encapsulated together with DNA molecules in efforts to build a minimal cell.[75] To monitor the protein synthesis reaction within the solid particles, fluorescent proteins (green fluorescent protein (GFP),[76,77] Venus,[78] etc.) has been in vitro synthesized and simultaneously measured by fluorescence microscopy. Kato et al.,[15] monitored the fluorescence of nascent GFP over the time inside oil droplets, these experiments allowed to quantify the cooperative action of this complex multi-enzyme system in real-time (Figure 7). These studies revealed a significant effect of particle size on the reaction kinetics; the protein was synthesized 5 times faster in smaller particles (20 μm) than in larger ones (71 μm). In this complex scenario, the translation rate of isolated immobilized ribosomes synthesizing GFP was locally recorded, and the observations demonstrated that local and bulk protein synthesis kinetics were similar.[79]

These single-particle studies of immobilized systems open new pathways to study the dynamics and the kinetics of biomanufacturing cascades spatially confined. Also, these techniques show a successful in operando monitoring of enzyme kinetics in consecutives reactions by using immobilized enzymes. Hence, the information provided shines light on the factors that locally affect the activity of immobilized enzymes. From these studies, we can evaluate the functional uniformity of one heterogeneous biocatalyst and understand the causes
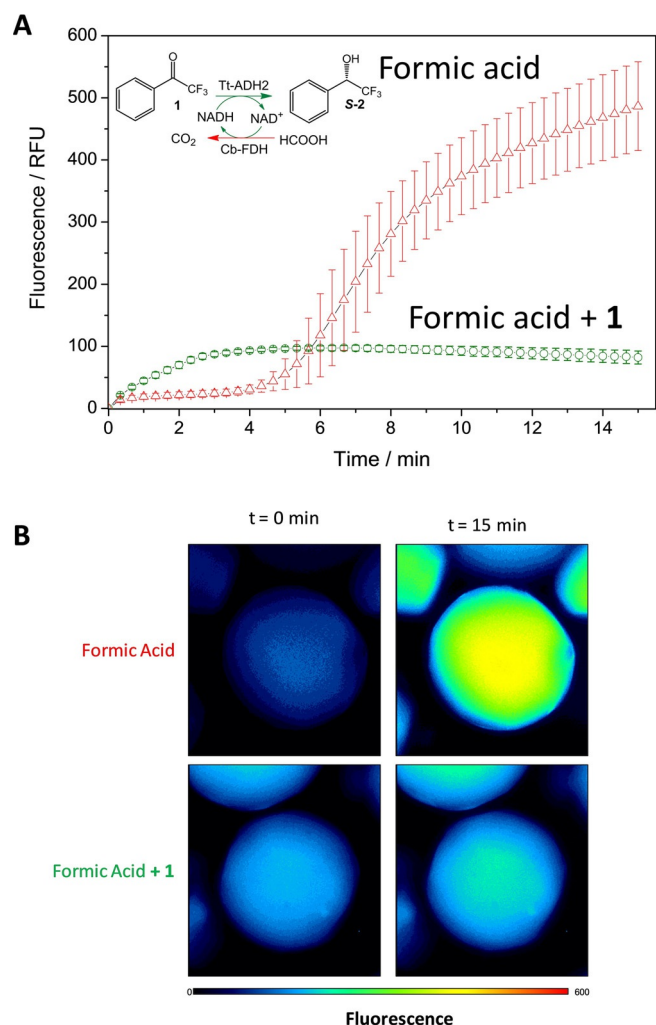
Figure 6. In operando analysis of the NAD^+/H utilization at single-particle level. Alcohol dehydrogenase from *Thermus thermophilus* (Tt-ADH2) and Formate dehydrogenase from *Candida boidinii* were irreversibly co-immobilized with the cofactor NAD^+ ionically absorbed on agarose beads (50–150 μm). The cofactor establishes an association/dissociation equilibrium that allows its internal diffusion inside the pores but avoids its external diffusion to the bulk. A) Single-particle monitoring during the redox biotransformation of the substrate formic acid (red △) and incorporating the NAD + recycling with 2,2,2-trifluoroacetophenone (1) (green ○).The reaction was monitored and the average fluorescence was quantified by measuring the autofluorescence of NADH at 460 nm for 15 minutes in 10 microbeads. B) Analysis of the fluorescence intensity of single beads from fluorescence microscopy images with (below) and without NAD + recycling (above), before (left) and after (right) the bioredox reactions were accomplished. Adpated from [69] with permission of Wiley.

Figure 7. Real-time monitoring cell-free protein synthesis in single particles. A) Distribution of GFP fluorescence synthesized in droplets with different sizes (smaller: 1, 2 and 3. Bigger: 4 and 5) at 3 h after encapsulation. B) Time-courses of the GFP concentration per unit volume, GFP in small ($R = 20$ μm; circles) and large ($R = 71$ μm; squares) droplets coated by a lipid layer. Triangles represent the negative control. Adapted from [15] with permission of Nature Publishing Group (NPG).

for the inefficient operation of certain enzymes under given reaction conditions.

4. Single-Particle Stability of Immobilized Enzymes and Proteins by using Spectroscopic Methods

Beside easing the downstream processing, the immobilization of enzymes also may stabilize them against certain reaction conditions underlying the industrial processes.[6,80,81] Normally, the immobilization provokes a structural rigidification in the
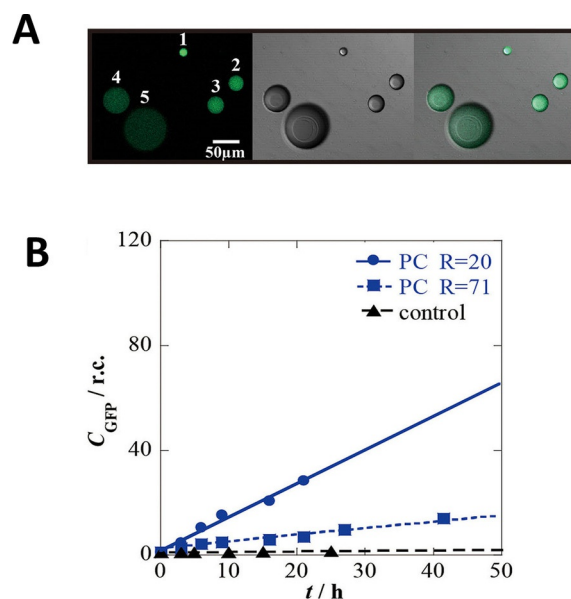
enzymes which may prevent them from the structural distortions triggered by inactivating agents such as high temperature, organic solvents,[82] etc. Thereupon, a better understanding of molecular processes that lead the protein rigidification may forecast the resulting stability and activity of enzymes upon the immobilization. This comprehension would be helpful for the fabrication and optimization of heterogeneous biocatalysts.

Conventionally, stability of immobilized enzymes is determined through bulk studies where the samples are incubated in presence of the corresponding inactivating agent, and the averaged enzymatic activity of each sample is measured at different inactivation times.[83] Additionally, microcalorimetric analysis, Trp-fluorescence studies and circular dichroism (CD)[33,84–86] can provide information about the structural stability of the immobilized enzymes. Nonetheless, these approaches lack the spatial resolution needed to grasp how the enzymes are stabilized at single-particle level. Fluorescence spectroscopy has lastly emerged as a powerful tool for single-particle studies of immobilized enzymes, aided by the outstanding advances in optical microscopy.[69,87–89] Orrego et al., combined fluorescence lifetime imaging and spatial-resolved fluorescence polarization to determine the fluorescence anisotropy of immobilized proteins as innovative strategy to analyze the stability[90] of immobilized proteins at single-particle level (Figure 8).

In this study, several EGFP variants were immobilized on porous agarose microbeads through different immobilization chemistries. The fluorescence data allowed determining the anisotropy of EGFP inside the beads with spatial resolution. Based on that information, the authors found a correlation
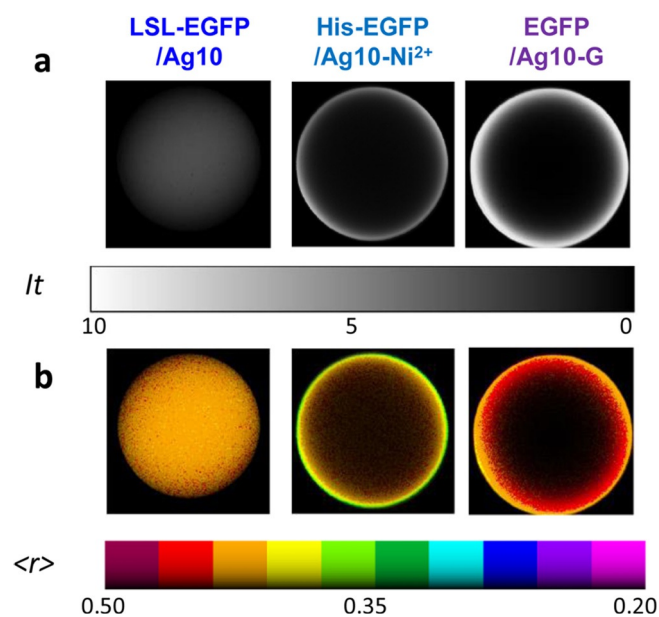
Figure 8. Single-particle analysis of the thermal stability of different EGFP variants (LSL-EGFP, His-EGFP and EGFP) immobilized on agarose beads (50–150 μm). AG10 is plain agarose, while AG10-Ni^{2+} and AG10-G are agarose beads activated with nickel chelates and aldehyde groups, respectively. LSL-EGFP is a lectin tagged enhanced fluorescent protein that is immobilized on AG10 through the lectin domain as spacer arm. His-EGFP is the same fluorescent protein tagged with a poly-histidine tag that allows its univalent and reversible immobilization on AG10-Ni^{2+} and EGFP is the untagged protein that is multivalently and irreversibly immobilized on AG10-G. A) Fluorescence intensity (grey scale) and B) fluorescence anisotropy (rainbow-like scale) of horizontal sections (80×80 μm) at the equator plane of the representative beads where EGFP variants are immobilized through different chemistries. The heterogeneous biocatalysts with higher anisotropy values were more thermally stable than those ones with lower anisotropy values. Adapted from [90] with permission of American Chemical Society.

between the protein flexibility and the thermal stability of the immobilized proteins. As conclusion, the fluorescence anisotropy reveals that proteins immobilized through chemistries that reduce the protein flexibility (high anisotropy values) are more thermostable than proteins that remain more flexible upon the immobilization.

On the other hand, atomic force microscopy (AFM) and spectroscopy (AFS) are broadly used to probe protein-surface interactions.[91–93] AFM is the only microscopic technique capable of creating topographical maps where visualizing biomolecules at the single-molecule level with sub-nanometer resolution in liquid.[93] Aissaoui et al.[94] have exploited AFM to image the aggregation of the enzymes immobilized on planar silanized surfaces (1×1 μm²) through different immobilization chemistries. They found a correlation between the size of the aggregates and the catalytic properties of the immobilized glucose 6-phosphate dehydrogenase. The smaller aggregates exhibit higher specific activity likely owing to less transport restrictions of the substrates, whereas the larger aggregates increase the thermal stability of the immobilized proteins, suggesting that such aggregation packs the 3D protein structure (Figure 9).

Beyond imaging, AFM can also perform spectroscopic studies to reveal the stiffness of those materials conjugated with biomolecules. This technique has been highly informative about the mechanical properties of the cell walls when displaying different proteins.[95] In the field of the immobilized enzymes, Gregurec et al.[96] applied single-bead atomic force spectroscopy to predict the thermal stability of several immobilized proteins. Here, the authors used a colloidal probe (1 μm) to indent 9 μm² surface of the single microbeads (120 μm) upon the immobilization of different oxidoreductases. The immobilization could be on line monitored in the microscope chamber because the conjugation of the proteins to the solid surface increased the stiffness of the whole bead. The immobilization chemistry affects differently to the mechanical properties of the beads upon the immobilization of the same protein. The results showed that irreversible and multivalent immobilization chemistries increase the stiffness of the microbeads and promote significant thermal stabilization of the immobilized enzymes. Remarkably, force spectroscopy studies arrived to the same conclusion that the studies based on fluorescence anisotropy of immobilized enzymes.[90]

Infrared (IR) techniques, including Fourier transform infrared (FTIR), attenuated total reflectance coupled with FTIR (ATR-FTIR) and sum-frequency generation spectroscopies have been widely exploited to evaluate the structural integrity of the enzymes upon the immobilization.[97–99] Monitoring the signal corresponding to the Amide I band of proteins, IR studies have revealed structural distortions of the immobilized enzymes, owing to the hydrophobicity of the surface, the crowding of the immobilized enzymes and their orientation; all these factors directly affect the thermal stability of the immobilized enzymes.[99] To gain spatial resolution, the immobilized enzymes have been analyzed with micro-FTIR spectroscopy; a powerful technique for in operando studies in heterogeneous chemical catalysis[10, 100] although its applications for heterogeneous biocatalysts are still on its infancy. The group of Prof. Lepore has exploited micro-FTIR to analyze the local conformation of glucose oxidase entrapped into a sol-gel matrix.[101–103] Beside the spatial distribution of the enzyme across the solid material, micro-FTIR unveils some local patches of structurally distorted glucose oxidase upon the immobilization, although the enzyme activity was macroscopically preserved. Additionally, micro-ATR/FTIR analysis of the same immobilized enzyme shows a temporal evolution of the infrared spectra within the solid particles that can be correlated to the enzyme inactivation over the time. Therefore, mapping properties such the aggregation and crowding states, the orientation, the flexibility and the stiffness of the immobilized proteins unmask relevant information that remains hidden in bulk experiments. Such information is vital to understand why immobilization often stabilizes enzymes and to further optimize the fabrication of heterogeneous biocatalysts. We envision the application of single-particle studies over the time under different reaction conditions to better understand the inactivation kinetics of the immobilized enzymes during the operational process.
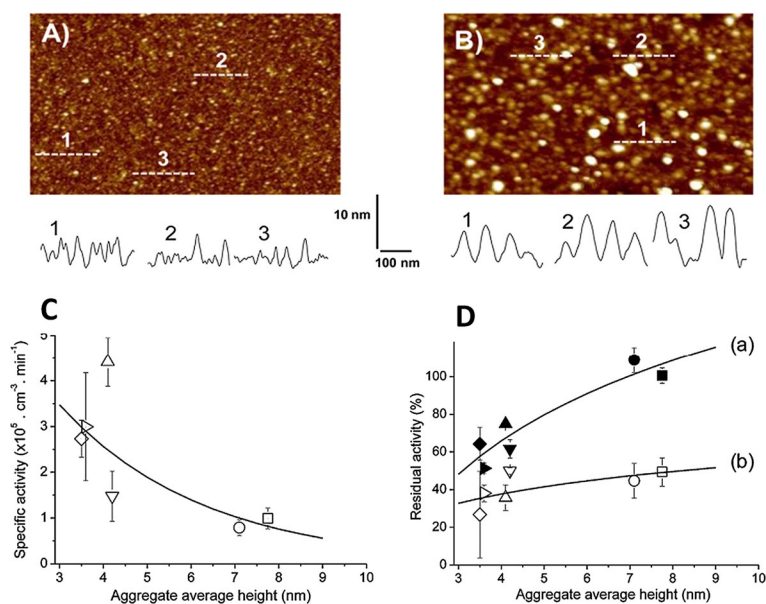
Figure 9. AFM analysis of enzymes immobilized on a silanized silicon oxide surface. AFM height images (peak force tapping mode, in phosphate buffer; z-scale 20 nm) of silanized silicon oxide A) after enzyme adsorption without previous linker treatment and B) after treatment with 1,4-phenylenendiisocyanate and subsequent enzyme adsorption. C) Specific activity of enzymes immobilized on silanized silicon surfaces as a function of the aggregate average heights determined by AFM, (Sil, $\diamond$) and using different cross-linkers: (1,4-phenylene diisocyanate, $\circ$), (1,4-phenylene diisothiocyanate, $\square$), (1,3-phenylene diisothiocyanate, $\triangle$), (Glutaraldehyde, $\triangledown$), and (Terephtalaldehyde, $\triangleright$). D) Thermal stability of immobilized enzymes on the same samples as a function of the aggregate average heights. Samples were incubated in a phosphate buffer for 1 hour at (a) 30 °C (closed symbols) and (b) 40 °C (open symbols). The percentage is relative to the original activity assayed without heating. Error bars correspond to the standard deviations of three independent experiments. The black curves are optical guidelines. Adapted from [94] with permission of American Chemical Society.

5. Spatio-Temporal Resolution of O_2 and pH Within Immobilized Enzymes

Enzymes immobilized on porous carriers suffer from diffusional effects, exhibiting substrate and product concentration gradients between the bulk liquid and the carrier surface;[18] pH and O_2 concentration are two variables particularly affected.[17,104] Both variables are important in biocatalysis since many enzymatic reactions create proton and O_2 gradients during the operational processes. The O_2 limitation lies in its low solubility in aqueous medium that originates a small driving force for O_2 supply into the solid biocatalyst; consequently, the low transfer rate compared to the enzymatic reaction rate leads to the dramatic depletion of the intraparticle O_2 concentration.[17,104] In this scenario, O_2-dependent heterogeneous biocatalysts offer a very low apparent activity. On the other hand, the pH gradients are created due to either partition effects within the solid material[105,106] or higher proton release/consumption enzymatic rates compared to the proton transfer rate. As consequence, the existence of internal pH gradients influences on the activity, stability and selectivity of the heterogeneous biocatalyst. In both cases, dissecting whether apparent catalytic properties are due to immobilization effects or to certain intraparticle environment[17,18] is necessary for the biocatalyst optimization.

Real-time determination of concentration gradients between the internal environment of the immobilized enzymes and the bulk solution is the best way to assess the significance of the diffusional limitations and to offer a better biocatalyst characterization.[17,18] There are many available solutions to measure O_2 and pH in homogeneous liquid phase with excellent spatio-temporal resolution.[107–110] However, the measurements near-surface or within solids particles are scarce since they present a high technological complexity and require specialized set-ups. The basic principle involves a luminescence indicator embedded within an analyte-permeable polymeric layer. This is further system-integrated by controlled deposition as in sensor spots and optical fiber tips, enabling different and often contactless optical read-outs. However, the methodology in the current form cannot be used to analyze the pH within solid porous.[110,111] The application for characterization of internal gradient measurements has two specific requirements. First, the luminescence dye and the enzyme should be properly co-immobilized within the same porous particle. Second, a read-out set-up should be established to provide measurements with suitable spatio-temporal resolution. A detailed description can be found in recent reviews.[17,18]

5.1. Resolution of Intraparticle O_2-Concentration

The quantification of spaced-averaged intraparticle O_2-concentrations has been applied to different enzyme porous carriers containing immobilized oxidases.[104,112,113] Polymethacrylate porous carriers were made O_2 sensitive by labeling with an O_2 sensitive luminophore and the analytical principle was the lifetime measurements based on application of the phase modulation technique.[104,112] The authors observed the formation of a large O_2 concentration gradient between the bulk and the intraparticle environment, which clearly indicates the O_2-supply limitations within the solid carrier.[104] The determination of oxygen gradients between homogeneous liquid phase and internal catalytic environment was performed simultaneously to the bulk determination of catalytic activity of immobilized oxidases[104,112,113] (Figure 10). These studies showed that the internally available O_2 concentration controls the catalytic effectiveness of heterogeneous biocatalyst.[104,112,113] Thus, a clear distinction between the effect of immobilization and substrate limitations was made possible.[18,112] Hence, the application of internal sensing enabled the optimization of geometrical properties (particle and pore sizes) of porous silica carriers to obtain biocatalytic process intensification through enhanced mass transport[113] (Figure 10 B–C).

Furthermore, internal measurements have proved the possibility of enhancement of intraparticle environment to reach conditions not achievable in liquid phase.[114] Intraparticle monitoring has allowed observing the release of internal oxygen from H_2O_2 using immobilized catalase, and conditions of
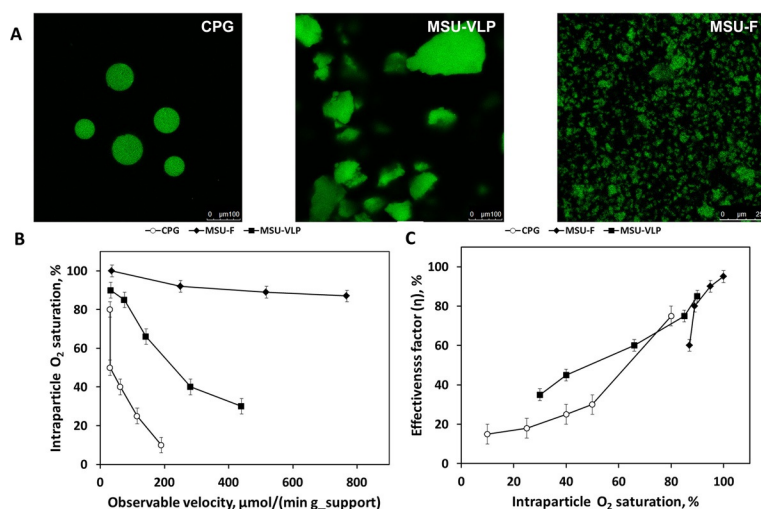
Figure 10. Effects of intraparticle oxygen on the activity of silica-based biocatalysts of a D-amino acid oxidase (DAAO) (A) Confocal fluorescence images of the enzyme DAAO immobilized on different porous silica supports with different particle sizes (from left to right, CPG (50–100 μm), MSU-VLP (5–140 μm) and MSU-F (3–7 μm). B) Dependence of the O$_2$ concentration inside the porous support (at apparent steady state) on the velocity of oxidation of D-methionine by the DAAO biocatalyst. C) Dependence of the effectiveness factor of the biocatalyst on the intraparticle O$_2$ concentration. All reactions were performed at 30°C using air-saturated potassium phosphate buffer (50 mM; pH 8.0). Adapted from [113] with permission of American Chemical Society.

intraparticle oxygen hypersaturation, not achievable by entraining gas into the porous material, have been detected.

5.2. Resolution of Intraparticle pH

Space-averaged intraparticle pH has been measured for the characterization of heterogeneous biocatalysts involving systematic biotransformations optimization, reaction modelling, reaction control and determination of kinetic and mass transfer parameters.[17,18,115–120] The hydrolysis of β-lactam substrates (which results in net proton formation) was studied by using FITC-labeled immobilized amidase in order to quantify the extent of the overall carrier acidification during the operation.[121] The internal pH was determined from pH-sensitive fluorescence intensity of FITC, showing a pH difference of 3 units between the bulk and the interior of the particles. This principle was applied to a fixed-bed reactor to monitor the internal pH across the reactor length. Combination of internal data and external data for reaction modelling was then possible and facilitates process understanding and targeted reactor selection.[121] Moreover, the determination of intrinsic kinetic parameters and mass transfer coefficients within porous materials is strongly supported when intraparticle concentrations are used instead of uniquely external data.[120] Recently, lifetime measurements (dual-lifetime referencing method, DLR) have improved the pH resolution[116,122] and served to study the influence of the carrier properties on the pH drop and monitor the reaction time course.

Moreover, DLR has been extended to apply new control strategies based on pH measurement within catalytic environment.[115] Finally, the internal pH has been used as key parameter to increase the lifetime of the immobilized enzyme under operational conditions.[117]

5.3. Internal Sensing at Single Particle Level

Opto-chemical sensing in combination with microscopy has the potential to determine internal pH and O$_2$ concentration in real-time and with spatial resolution (Figure 11 A). However, only a handful of examples have been reported. Spieß and colleagues performed a pioneer study to characterize different catalysts of immobilized penicillin G amidase by using referenced fluorescence intensity measurements of internal pH in a CLSM.[123] Their study was seminal in demonstrating the importance of internal pH to optimize the enzyme immobilization. They showed that internal pH alters the selectivity of the immobilized amidase, implying the need to select carriers and immobilization chemistries that provide an *optimum internal environment*. Huang and colleagues applied similar analytical techniques to determine pH gradients in biocatalytic membranes containing immobilized glucose oxidase. A pH drop resulted in this case from the oxidation of D-glucose into D-gluconic acid.[124] The application of fluorescence lifetime[125] or multiphoton laser scanning microscopy[126,127] solve some of the known limitations of measurements in CLSM.[17,18] Consequently, these techniques have been applied to the spatial resolution of internal pH inside hydrogels particles (1.5 mm) where the events of substrate diffusion and enzymatic reactions were resolved by elucidating the local concentration gradients through the catalytic particle.[127] Unfortunately, lifetime or referenced
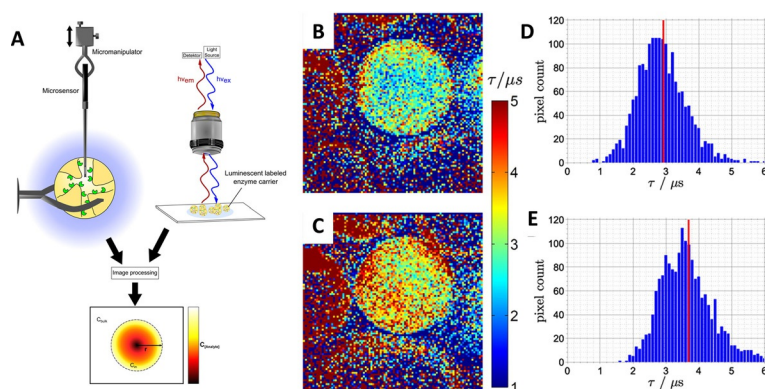

Figure 11. A) Opto-chemical sensing of O$_2$ with spatial resolution. Whereas a microelectrode should be placed at variable positions inside the carrier, microscopic techniques allow non-invasive measurement. Image processing is needed to obtain spatially resolved concentration data. B–E) Luminescence lifetime images of beads with immobilized enzyme and Ru(dpp)3, imaged under flow without (B,D) and with (C,E) substrate, resulting in different oxygen concentrations. D,E) Pixel lifetime distributions of the beads shown in (B) and (C) with the mean value marked by a red line. Adapted from [17] and [128] with permision of Cell Press and American Chemical Society.

measurements in CLSM depends on high-cost instrumentation that cannot be adapted to real-life reactor configurations and has limited throughput capacity, this has probably limited their application for heterogeneous biocatalyst at single-particle level.

The spatio-temporal mapping of O_2 has been restricted due to the difficulty of applying lifetime imaging in the range of microsecond. Recently, a new method based on variable excitation time determined by the scanning velocity was implemented in a CLSM (Figure 11). The method allows phosphorescence lifetime imaging and thus spatio-temporal resolution within porous enzyme carriers.[128] It was applied for the study of the oxygen depletion within particles containing immobilized lactate oxidase under packed-bed reactor configuration.

Summary and Outlook

Immobilized enzymes have been widely exploited because they work as heterogeneous biocatalysts, allowing their recovery and reutilization and easing the downstream processing once the chemical reactions are completed. Although immobilized enzymes have been utilized since decades, they are still considered as a "black box" where the effects of the surface on the enzyme properties are poorly understood at microscopic level. The lack of that information has limited the rational design and optimization of more efficient heterogeneous biocatalyst. In this Concept article, we have reviewed how single-particle studies provide fundamental information about the functionality, the structural integrity and the microenvironments of the enzymes immobilized on solid materials. In the last three decades, the single-particle studies of immobilized enzymes have advanced in the characterization of heterogeneous biocatalysts eliciting information that is masked in macroscopic studies based on bulk experiments. The latest advances in spectroscopic techniques with spatial resolution have boosted the characterization of immobilized enzymes at single-particle level, which allows better understanding the operational performance of the enzymes bound to solid materials. In this article, we have given examples of how single-particle studies image the spatial distribution of the enzymes, the substrate diffusion and the reaction kinetics across the solid surfaces, the structural integrity and mobility of the immobilized enzymes inside the solid particles, and the pH and O_2 internal gradients. All these data provide vital information to unveil the optimal localization of immobilized enzymatic systems to more efficiently catalyze chemical reactions, the optimal attachment between the solid surface and the enzyme to yield more thermostable heterogeneous biocatalysts, and the optimal carrier architecture to reduce the mass transport limitations for reactants and oxygen. All this information contributes to develop more rational, reliable and reproducible proceedings when fabricating heterogeneous biocatalysts.

Nevertheless, there is still a long way to elicit structural and functional properties of immobilized enzymes on porous materials at the nanometric scale, an even longer at atomic-scale. Additionally, in operando studies at single-particle level must gain in temporal resolution to study the reactants utilization

and the protein conformational changes during the enzyme catalysis at very short-times (ns-ms). Likewise, we need to expand these techniques to monitor enzyme properties in more complex chemical process, including chemo-enzymatic ones, and more sophisticated operational design like flow-(micro) reactors. Therefore, the fabrication of extremely ordered materials and the emergence of high-resolution techniques for the solid-state will open new windows of understanding for this specialized form of biocatalysis.

Conflict of interest

The authors declare no conflict of interest.

[1] S. Kauthale, S. Tekale, M. Damale, J. Sangshetti, R. Pawar, *Bioorg. Med. Chem. Lett.* **2017**, *27*, 3891–3896.

[2] P. Panas, C. Lopes, M. O. Cerri, S. P. M. Ventura, V. C. Santos-Ebinuma, J. F. B. Pereira, *Fluid Phase Equilib.* **2017**, *450*, 42–50.

[3] R. DiCosimo, J. McAuliffe, A. J. Poulose, G. Bohlmann, *Chem. Soc. Rev.* **2013**, *42*, 6437–6474.

[4] A. S. Bommarius, M. F. Paye, *Chem. Soc. Rev.* **2013**, *42*, 6534–6565.

[5] A. Liese, L. Hilterhaus, *Chem. Soc. Rev.* **2013**, *42*, 6236–6249.

[6] R. C. Rodrigues, C. Ortiz, A. Berenguer-Murcia, R. Torres, R. Fernandez-Lafuente, *Chem. Soc. Rev.* **2013**, *42*, 6290–6307.

[7] S. Cantone, V. Ferrario, L. Corici, C. Ebert, D. Fattor, P. Spizzo, L. Gardossi, *Chem. Soc. Rev.* **2013**, *42*, 6262–6276.

[8] A. Pellis, S. Cantone, C. Ebert, L. Gardossi, *N. Biotechnol.* **2018**, *40*, 154–169.

[9] J. Frenken, I. Groot in *Springer Series in Chemical Physics.*, Vol.114 (Eds.: J. Frenken, I.Groot), Springer International Publishing, Berlin, Germany, **2017**.

[10] K. F. Kalz, R. Kraehnert, M. Dvoyashkin, R. Dittmeyer, R. Gläser, U. Krewer, K. Reuter, J.-D. Grunwaldt, *ChemCatChem* **2017**, *9*, 17–29.

[11] K. Morgan, J. Touitou, J.-S. Choi, C. Coney, C. Hardacre, J. A. Pihl, C. E. Stere, M.-Y. Kim, C. Stewart, A. Goguet, W. P. Partridge, *ACS Catal.* **2016**, *6*, 1356–1381.

[12] W. Neto, M. Schürmann, L. Panella, A. Vogel, J. M. Woodley, *J. Mol. Catal. B* **2015**, *117*, 54–61.

[13] I. L. C. Buurmans, B. M. Weckhuysen, *Nat. Chem.* **2012**, *4*, 873–886.

[14] J. S. Weltz, D. K. Schwartz, J. L. Kaar, *ACS Nano* **2016**, *10*, 730–738.

[15] A. Kato, M. Yanagisawa, Y. T. Sato, K. Fujiwara, K. Yoshikawa, *Sci. Rep.* **2012**, *2*, 283.

[16] H. Takahashi, K. Emoto, M. Dubey, D. G. Castner, D. W. Grainger, *Adv. Funct. Mater.* **2008**, *18*, 2079–2088.

[17] J. M. Bolivar, T. Consolati, T. Mayr, B. Nidetzky, *Trends Biotechnol.* **2013**, *31*, 194–203.

[18] J. M. Bolivar, I. Eisl, B. Nidetzky, *Catal. Today* **2016**, *259*, 66–80.

[19] A. Gershenson, *Curr. Opin. Chem. Biol.* **2009**, *13*, 436–442.

[20] L. Tamborini, P. Fernandes, F. Paradisi, F. Molinari, *Trends Biotechnol.* **2018**, *36*, 73–88.

[21] T. C. Logan, D. S. Clark, T. B. Stachowiak, F. Svec, J. M. J. Fréchet, *Anal. Chem.* **2007**, *79*, 6592–6598.

[22] A. D. Balomenos, P. Tsakanikas, Z. Aspridou, A. P. Tampakaki, K. P. Koutsoumanis, E. S. Manolakos, *BMC Syst. Biol.* **2017**, *11*, 43.

[23] J. van Roon, R. Beeftink, K. Schroën, H. Tramper, *Curr. Opin. Biotechnol.* **2002**, *13*, 398–405.

[24] A. Ciaccafava, P. Infossi, M. Ilbert, M. Guiral, S. Lecomte, M. T. Giudici-Orticoni, E. Lojou, *Angew. Chem.* **2012**, *124*, 977 – 980.

[25] W. Ott, M. A. Jobst, C. Schoeler, H. E. Gaub, M. A. Nash, *J. Struct. Biol.* **2017**, *197*, 3 – 12.

[26] A. Hoenger, *Protoplasma* **2014**, *251*, 417 – 427.

[27] A. Mayoral, R. Arenal, V. Gascón, C. Márquez-Álvarez, R. M. Blanco, I. Díaz, *ChemCatChem* **2013**, *5*, 903 – 909.

[28] B. Chen, J. Hu, E. M. Miller, W. Xie, M. Cai, R. A. Gross, *Biomacromolecules* **2008**, *9*, 463 – 471.

[29] F. López-Gallego, L. Yate, *Chem. Commun.* **2015**, *51*, 8753 – 8756.

[30] D. Hormigo, I. de la Mata, C. Acebal, M. Arroyo, *Bioresour. Technol.* **2010**, *101*, 4261 – 4268.

[31] D. Hormigo, I. De La Mata, M. Castillón, C. Acebal, M. Arroyo, *Biocatal. Biotransform.* **2009**, *27*, 271 – 281.

[32] E. A. Permyakov, *Biophys. J.* **1994**, *67*, 5.

[33] F. Secundo, *Chem. Soc. Rev.* **2013**, *42*, 6250 – 6261.

[34] M. W. Davidson, R. E. Campbell, *Nat. Methods* **2009**, *6*, 713 – 717.

[35] P. Torres, A. Datla, V. W. Rajasekar, S. Zambre, T. Ashar, M. Yates, M. L. Rojas-Cervantes, O. Calero-Rueda, V. Barba, M. J. Martínez, A. Ballesteros, F. J. Plou, *Catal. Commun.* **2008**, *9*, 539 – 545.

[36] J. M. Bolivar, A. Hidalgo, L. Sánchez-Ruiloba, J. Berenguer, J. M. Guisán, F. López-Gallego, *J. Biotechnol.* **2011**, *155*, 412 – 420.

[37] F. López-Gallego, I. Acebrón, J. M. Mancheño, S. Raja, M. P. Lillo, J. M. Guisán Seijas, *Bioconjugate Chem.* **2012**, *23*, 565 – 573.

[38] C. P. Toseland, *J. Chem. Biol.* **2013**, *6*, 85 – 95.

[39] N. M. Thomson, S. Sangiambut, K. Ushimaru, E. Sivaniah, T. Tsuge, *ACS Biomater. Sci. Eng.* **2017**, *3*, 3076 – 3082.

[40] J. Rocha-Martín, B. de las Rivas, R. Muñoz, J. M. Guisán, F. López-Gallego, *ChemCatChem* **2012**, *4*, 1279 – 1288.

[41] Z. Li, Y. Zhang, Y. Su, P. Ouyang, J. Ge, Z. Liu, *Chem. Commun.* **2014**, *50*, 12465 – 12468.

[42] H. Harada, A. Onoda, T. Uchihashi, H. Watanabe, N. Sunagawa, M. Samejima, K. Igarashi, T. Hayashi, *Chem. Sci.* **2017**, *8*, 6561 – 6565.

[43] K. Blank, G. De Cremer, J. Hofkens, *Biotechnol. J.* **2009**, *4*, 465 – 479.

[44] X. Ji, P. Wang, Z. Su, G. Ma, S. Zhang, *J. Mater. Chem. B* **2014**, *2*, 181 – 190.

[45] H. Bäumler, R. Georgieva, *Biomacromolecules* **2010**, *11*, 1480 – 1487..

[46] W. E. Moerner, D. P. Fromm, *Rev. Sci. Instrum.* **2003**, *74*, 3597 – 3619.

[47] P. Tinnefeld, M. Sauer, *Angew. Chem. Int. Ed.* **2005**, *44*, 2642 – 2671; *Angew. Chem.* **2005**, *117*, 2698 – 2728.

[48] P. Turunen, A. E. Rowan, K. Blank, *FEBS Lett.* **2014**, *588*, 3553 – 3563.

[49] E. D'Aguanno, E. Altamura, F. Mavelli, A. Fahr, P. Stano, P. L. Luisi, *Life* **2015**, *5*, 969 – 996.

[50] T. Laursen, A. Singha, N. Rantzau, M. Tutkus, J. Borch, P. Hedegård, D. Stamou, B. L. Møller, N. S. Hatzakis, *ACS Chem. Biol.* **2014**, *9*, 630 – 634.

[51] H. M. Piwonski, M. Goomanovsky, D. Bensimon, A. Horovitz, G. Haran, *Proc. Natl. Acad. Sci. USA* **2012**, *109*, E1437 – E1443.

[52] K. Velonia, O. Flomenbom, D. Loos, S. Masuo, M. Cotlet, Y. Engelborghs, J. Hofkens, A. E. Rowan, J. Klafter, R. J. M. Nolte, F. C. de Schryver, *Angew. Chem. Int. Ed.* **2005**, *44*, 560 – 564; *Angew. Chem.* **2005**, *117*, 566 – 570.

[53] L. Wang, P. Wen, X. Liu, Y. Zhou, M. Li, Y. Huang, L. Geng, S. Mann, X. Huang, *Chem. Commun.* **2017**, *53*, 8537 – 8540.

[54] K. P. F. Janssen, G. De Cremer, R. K. Neely, A. V. Kubarev, J. Van Loon, J. A. Martens, D. E. De Vos, M. B. J. Roeffaers, J. Hofkens, *Chem. Soc. Rev.* **2014**, *43*, 990 – 1006.

[55] J. Eid, A. Fehr, J. Gray, K. Luong, J. Lyle, G. Otto, P. Peluso, D. Rank, P. Baybayan, et al., *Science* **2009**, *323*, 133 – 138.

[56] A. Houde, A. Kademi, D. Leblanc, *Appl. Biochem. Biotechnol.* **2004**, *118*, 155 – 170.

[57] N. Gao, T. Tian, J. Cui, W. Zhang, X. Yin, S. Wang, J. Ji, G. Li, *Angew. Chem. Int. Ed.* **2017**, *56*, 3880 – 3885; *Angew. Chem.* **2017**, *129*, 3938 – 3943.

[58] C.-A. Liao, Q. Wu, Q.-C. Wei, Q.-G. Wang, *Chem. Eur. J.* **2015**, *21*, 12620 – 12626.

[59] C. A. Mandon, L. J. Blum, C. A. Marquette, *Anal. Chem.* **2016**, *88*, 10767 – 10772.

[60] R. J. R. W. Peters, M. Marguet, S. Marais, M. W. Fraaije, J. C. M. van Hest, S. Lecommandoux, *Angew. Chem. Int. Ed.* **2014**, *53*, 146 – 150; *Angew. Chem.* **2014**, *126*, 150 – 154.

[61] W. Kroutil, E.-M. Fischereder, C. S. Fuchs, H. Lechner, F. G. Mutti, D. Pressnitz, A. Rajagopalan, J. H. Sattler, R. C. Simon, E. Siirola, *Org. Process Res. Dev.* **2013**, *17*, 751 – 759.

[62] B. M. Nestl, S. C. Hammer, B. A. Nebel, B. Hauer, *Angew. Chem. Int. Ed.* **2014**, *53*, 3070 – 3095; *Angew. Chem.* **2014**, *126*, 3132 – 3158.

[63] R. Sigrist, B. Zucoloto da Costa, A. J. Marsaioli, L. G. de Oliveira, *Biotechnol. Adv.* **2015**, *33*, 394 – 411.

[64] Y.-W. Tan, H. Yang, *Phys. Chem. Chem. Phys.* **2011**, *13*, 1709 – 1721.

[65] H. Yang, G. Luo, P. Karnchanaphanurach, T.-M. Louie, I. Rech, S. Cova, L. Xun, X. S. Xie, *Science* **2003**, *302*, 262 – 266.

[66] K. Busch, J. Piehler, H. Fromm, *Biochemistry* **2000**, *39*, 10110 – 10117.

[67] A. I. Benítez-Mateos, E. San Sebastián, N. Ríos-Lombardía, F. Morís, J. González-Sabín, F. Lopez-Gallego, *Chem. Eur. J.* **2017**, *23*, 16843 – 16852.

[68] J. G. Dorsey, W. T. Cooper, B. A. Siles, J. P. Foley, H. G. Barth, *Anal. Chem.* **1996**, *68*, 515 – 568.

[69] S. Velasco-Lozano, A. I. Benítez-Mateos, F. López-Gallego, *Angew. Chem. Int. Ed.* **2017**, *56*, 771 – 775; *Angew. Chem.* **2017**, *129*, 789 – 793.

[70] J. C. O'Brien, J. Shumaker-Parry, R. C. Engstrom, *Anal. Chem.* **1998**, *70*, 1307 – 1311.

[71] S. Garny, N. Beeton-Kempen, I. Gerber, J. Verschoor, J. Jordaan, *Enzyme Microb. Technol.* **2016**, *85*, 71 – 81.

[72] F. G. Mutti, T. Knaus, N. S. Scrutton, M. Breuer, N. J. Turner, *Science* **2015**, *349*, 1525 – 1529.

[73] J. H. Sattler, M. Fuchs, F. G. Mutti, B. Grischek, P. Engel, J. Pfeffer, J. M. Woodley, W. Kroutil, *Angew. Chem. Int. Ed.* **2014**, *53*, 14153 – 14157; *Angew. Chem.* **2014**, *126*, 14377 – 14381.

[74] M. Yu, D. Liu, L. Sun, J. Li, Q. Chen, L. Pan, J. Shang, S. Zhang, W. Li, *Int. J. Biol. Macromol.* **2017**, *103*, 424 – 434.

[75] H. Jia, M. Heymann, F. Bernhard, P. Schwille, L. Kai, *N. Biotechnol.* **2017**, *39*, 199 – 205.

[76] F. Caschera, J. W. Lee, K. K. Y. Ho, A. P. Liu, M. C. Jewett, *Chem. Commun.* **2016**, *52*, 5467 – 5469.

[77] F. Caschera, V. Noireaux, *Artif. Life* **2016**, *22*, 185 – 195.

[78] A. C. Spencer, P. Torre, S. S. Mansy, *J. Vis. Exp.* **2013**, *80*, e51304.

[79] S. Uemura, R. Iizuka, T. Ueno, Y. Shimizu, H. Taguchi, T. Ueda, J. D. Puglisi, T. Funatsu, *Nucleic Acids Res.* **2008**, *36*, e70 – e70.

[80] C. Mateo, J. M. Palomo, G. Fernandez-Lorente, J. M. Guisan, R. Fernandez-Lafuente, *Enzyme Microb. Technol.* **2007**, *40*, 1451 – 1463.

[81] T. L. Ogorzalek, S. Wei, Y. Liu, Q. Wang, C. L. Brooks, Z. Chen, E. N. G. Marsh, *Langmuir* **2015**, *31*, 6145 – 6153.

[82] R. A. Sheldon, S. van Pelt, *Chem. Soc. Rev.* **2013**, *42*, 6223 – 6235.

[83] A. Sadana, *Biotechnol. Adv.* **1988**, *6*, 349-IN342.

[84] N. J. Greenfield, *Nat. Protoc.* **2006**, *1*, 2891 – 2899.

[85] S. M. Kelly, N. C. Price, *Curr. Protoc. Protein Sci.* **2006**, 20.10.

[86] S. H. North, C. R. Taitt, *Peptide Microarrays: Methods and Protocols*. New York, NY, Springer New York, **2016**.

[87] A. Ljunglöf, R. Hjorth, *J. Chromatogr. A* **1996**, *743*, 75 – 83.

[88] P. S. Nabavi Zadeh, K. A. Mallak, N. Carlsson, B. Åkerman, *Anal. Biochem.* **2015**, *476*, 51 – 58.

[89] M. C. Pinto, P. Macías, *Biotechnol. Tech.* **1995**, *9*, 481 – 486.

[90] A. H. Orrego, C. García, J. M. Mancheño, J. M. Guisán, M. P. Lillo, F. López-Gallego, *J. Phys. Chem. B* **2016**, *120*, 485 – 491.

[91] G. Binnig, C. F. Quate, C. Gerber, *Phys. Rev. Lett.* **1986**, *56*, 930 – 933.

[92] L. Dušan, *J. Serb. Chem. Soc.* **2004**, *69*, 14.

[93] C. Marcuello, R. de Miguel, C. Gómez-Moreno, M. Martínez-Júlvez, A. Lostao, *Protein Eng. Des. Sel.* **2012**, *25*, 715 – 723.

[94] N. Aissaoui, L. Bergaoui, S. Boujday, J.-F. Lambert, C. Méthivier, J. Landoulsi, *Langmuir* **2014**, *30*, 4066 – 4077.

[95] L. Arnal, D. O. Serra, N. Cattelan, M. F. Castez, L. Vázquez, R. C. Salvarezza, O. M. Yantorno, M. E. Vela, *Langmuir* **2012**, *28*, 7461 – 7469.

[96] D. Gregurec, S. Velasco-Lozano, S. E. Moya, L. Vazquez, F. Lopez-Gallego, *Soft Matter* **2016**, *12*, 8718 – 8725.

[97] S. E. Glassford, B. Byrne, S. G. Kazarian, *Biochim. Biophys. Acta Proteins Proteomics* **2013**, *1834*, 2849 – 2858.

[98] A. Márquez, K. Kocsis, G. Zickler, G. R. Bourret, A. Feinle, N. Hüsing, M. Himly, A. Duschl, T. Berger, O. Diwald, *J. Nanobiotechnology* **2017**, *15*, 55.

[99] M. M. Schroeder, Q. Wang, S. Badieyan, Z. Chen, E. N. G. Marsh, *Langmuir* **2017**, *33*, 7152 – 7159.

[100] A. Davó-Quiñonero, A. Bueno-López, D. Lozano-Castelló, A. J. McCue, J. A. Anderson, *ChemCatChem* **2016**, *8*, 1905–1908.

[101] I. Delfino, M. Portaccio, B. D. Ventura, D. G. Mita, M. Lepore, *Mater. Sci. Eng. C* **2013**, *33*, 304–310.

[102] M. Portaccio, B. Della Ventura, D. G. Mita, N. Manolova, O. Stoilova, I. Rashkov, M. Lepore, *J. Sol-Gel Sci. Technol.* **2011**, *57*, 204–211.

[103] M. Portaccio, R. Esposito, I. Delfino, M. Lepore, *J. Sol-Gel Sci. Technol.* **2014**, *71*, 580–588.

[104] J. M. Bolivar, T. Consolati, T. Mayr, B. Nidetzky, *Biotechnol. Bioeng.* **2013**, *110*, 2086–2095.

[105] X. Sun, J. Xie, J. Xu, D. A. Higgins, K. L. Hohn, *Langmuir* **2015**, *31*, 5667–5675.

[106] A. Yamaguchi, M. Namekawa, T. Kamijo, T. Itoh, N. Teramae, *Anal. Chem.* **2011**, *83*, 2939–2946.

[107] M. Barczak, C. McDonagh, D. Wencel, *Microchim. Acta* **2016**, *183*, 2085–2109.

[108] P. Gruber, M. P. C. Marques, N. Szita, T. Mayr, *Lab Chip* **2017**, *17*, 2693–2712.

[109] M. Quaranta, S. M. Borisov, I. Klimant, *Bioanal. Rev.* **2012**, *4*, 115–157.

[110] X.-d. Wang, O. S. Wolfbeis, *Chem. Soc. Rev.* **2014**, *43*, 3666–3761.

[111] D. Wencel, T. Abel, C. McDonagh, *Anal. Chem.* **2014**, *86*, 15–29.

[112] J. M. Bolivar, S. Schelch, T. Mayr, B. Nidetzky, *ChemCatChem* **2014**, *6*, 981–986.

[113] J. M. Bolivar, S. Schelch, T. Mayr, B. Nidetzky, *ACS Catal.* **2015**, *5*, 5984–5993.

[114] J. M. Bolivar, S. Schelch, M. Pfeiffer, B. Nidetzky, *J. Mol. Catal. B* **2016**, *134*, 302–309.

[115] J. Begemann, A. C. Spiess, *Biotechnol. J.* **2015**, *10*, 1822–1829.

[116] C. Boniello, T. Mayr, J. M. Bolivar, B. Nidetzky, *BMC Biotechnol.* **2012**, *12*, 11.

[117] H. Luo, L. Zhu, Y. Chang, X. Liu, Z. Liu, H. Sun, X. Li, H. Yu, Z. Shen, *Bioresour. Technol.* **2017**, *223*, 157–165.

[118] A. Spieß, R.-C. Schlothauer, J. Hinrichs, B. Scheidat, V. Kasche, *Biotechnol. Bioeng.* **1999**, *62*, 267–277.

[119] C. Thörn, N. Carlsson, H. Gustafsson, K. Holmberg, B. Åkerman, L. Olsson, *Microporous Mesoporous Mater.* **2013**, *165*, 240–246.

[120] T. Zahel, C. Boniello, B. Nidetzky, *Process Biochem.* **2013**, *48*, 593–604.

[121] A. Spieß, R. Schlothauer, J. Hinrichs, B. Scheidat, V. Kasche, *Biotechnol. Bioeng.* **1999**, *62*, 267–277.

[122] C. Boniello, T. Mayr, I. Klimant, B. Koenig, W. Riethorst, B. Nidetzky, *Biotechnol. Bioeng.* **2010**, *106*, 528–540.

[123] A. C. Spiess, V. Kasche, *Biotechnol. Prog.* **2001**, *17*, 294–303.

[124] H. Y. Huang, J. Shaw, C. Yip, X. Y. Wu, *Pharm. Res.* **2008**, *25*, 1150–1157.

[125] E. Kuwana, F. Liang, E. M. Sevick-Muraca, *Biotechnol. Prog.* **2004**, *20*, 1561–1566.

[126] T. Schwendt, C. Michalik, M. Zavrel, A. Dennig, A. C. Spiess, R. Poprawe, C. Janzen, *Appl. Spectrosc.* **2010**, *64*, 720–726.

[127] M. Zavrel, C. Michalik, T. Schwendt, T. Schmidt, M. Ansorge-Schumacher, C. Janzen, W. Marquardt, J. Büchs, A. C. Spiess, *Chem. Eng. Sci.* **2010**, *65*, 2491–2499.

[128] Z. Petrášek, J. M. Bolivar, B. Nidetzky, *Anal. Chem.* **2016**, *88*, 10736–10743.